BimD/SPO76 is at the interface of cell cycle progression, chromosome morphogenesis, and recombination

Diana van Heemst*†, Etta Käfer‡, Tricia John‡, Christa Heyting†, Mirjam van Aalderen†, and Denise Zickler*§

*Institut de Génétique et Microbiologie, UMR 8621, Université Paris Sud, 91405 Orsay Cedex, France; †Department of Genetics, Wageningen University, 6703 HA Wageningen, The Netherlands; and ‡Department of Molecular Biology and Biochemistry, Simon Fraser University, Burnaby, BC, Canada V5A 1S6

Communicated by Nancy Kleckner, Harvard University, Cambridge, MA, February 21, 2001 (received for review November 13, 2000)

BIMD of *Aspergillus nidulans* belongs to a highly conserved protein family implicated, in filamentous fungi, in sister-chromatid cohesion and DNA repair. We show here that BIMD is chromosome associated at all stages, except from late prophase through anaphase, during mitosis and meiosis, and is involved in several aspects of both programs. First, *bimD*$^+$ function must be executed during S through M. Second, in *bimD6* germlings, mitotic nuclear divisions and overall cellular program occur more rapidly than in wild type. Thus, BIMD, an abundant chromosomal protein, is a negative regulator of normal cell cycle progression. Third, *bimD6* reduces the level of mitotic interhomolog recombination but does not alter the ratio between crossover and noncrossover outcomes. Moreover, *bimD6* is normal for intrachromosomal recombination. Therefore, BIMD is probably not involved in the enzymology of recombinational repair *per se*. Finally, during meiosis, staining of the *Sordaria* ortholog Spo76p delineates robust chromosomal axes, whereas BIMD stains all chromatin. *SPO76* and *bimD* are functional homologs with respect to their roles in mitotic chromosome metabolism but not in meiosis. We propose that BIMD exerts its diverse influences on cell cycle progression as well as chromosome morphogenesis and recombination by modulating chromosome structure.

Cell division results from an integrated sequence of events, occurring in an orderly way, to ensure faithful transmission of the genetic information to the next generation. As part of this process, chromosome morphogenesis and progression of other cellular events occur coordinately. The exact relationship between the chromosomal cycle and cell cycle regulation remains poorly understood.

It is clear that cell cycle molecules influence chromosome behavior (review in ref. 1). The opposite is likely also true, not only during "checkpoint" responses but also in a normal unperturbed mitotic cell (see review, ref. 2). Notably, several key chromosomal proteins have been implicated in regulation of cell cycle progression. The human homologs of the Pds1/Cut2p securin and of the Spo76/BIMD/AS3 family of chromosomal proteins have been identified as possible tumor suppressors (3, 4). Correspondingly, androgen-induced G_1 arrest in human is mediated by up-regulation of *AS3* (5), and overexpression of *bimD* confers arrest in G_1 (6). Also, overexpression of the mouse homolog of the Mcd1/Scc1/Rad21p cohesin leads to inhibition of fibroblast proliferation (7).

The evolutionarily conserved Spo76 family includes Spo76p of *Sordaria macrospora* (4, 8), BIMD of *Aspergillus nidulans* (6), Pds5p of budding yeast (9, 10), as well as AS3 and hPDS5 of human (5, 11). Spo76p is essential for mitotic and meiotic chromosome morphogenesis and is associated with the chromosomes in both programs (4). All three fungal proteins are implicated in maintenance of sister-chromatid cohesion (4, 6, 8–10). Moreover, the mitotic catastrophe defect of *bimD6* is suppressed by mutations in the *Aspergillus* homolog of the cohesin Smc3 (12).

To gain further insight into the function and behavior of Spo76 family proteins with respect to both chromosome morphogenesis and regulation of cell cycle progression, we have used the filamentous fungus *A. nidulans*, which is particularly well suited for such analyses (13, 14). We have followed the chromosomal localization of BIMD in mitosis and meiosis. In the mitotic program, we have analyzed execution points and examined effects of *bimD6* on cell cycle progression and spontaneous recombination. Finally, we tested *bimD* and *SPO76* for heterologous complementation of mutant defects.

Materials and Methods

Strains. Because all laboratory strains of the homothallic *A. nidulans* are derived from a single nucleus, they are essentially isogenic (15). All *bimD6* strains used were progeny of strain D6.9 *riboA1*; *sC12*; *bimD6 pyroA4* (6) and are available (as A1063) from the Fungal Genetics Stock Center (University of Kansas Medical Center, Kansas City, KS). A cross of A1064 (F1 of A1063) to FGSC strain A733, *pyrG89*; *wA3*; *pyroA4* produced six strains: *pyroA4*, *wA3*; *pyroA4*, *pyrG89*; *pyroA4*, and three corresponding *bimD6* strains. Quantitative assessment of complementation by *SPO76* was performed in two additional *pyrG89 bimD6* strains (A1061 and A1062). The recipient strain for transformation of *S. macrospora* was *spo76–1* (4). For *bimD6* strains, permissive temperature was 25 or 30°C, and restrictive temperature was 42°C.

Mitotic allelic recombination in *adE8/adE20* (16) was examined in isogenic strains homozygous for *bimD*$^+$ or *bimD6* (for genotypes, see Table 2, which is published as supplemental data on the PNAS web site, www.pnas.org). For intrachromosomal recombination, suitable *pyrG89*; *bimD6* and *pyrG89*; *uvsC114 benA* duplication strains were obtained by crosses to strain IS88 (17).

Media and Genetic Procedures. Standard *Aspergillus* media and genetic techniques (15), modifications of the media, methods of mitotic mapping, congenic strain construction (18), and procedures for genetic analysis of DNA repair mutants and of their effects on mitotic recombination in diploids were all as described previously (16). For tests of intrachromosomal recombination, the *benA* interrupted duplication system (17) was adapted for visual assessment of recombination frequencies.

Transformation. The *Aspergillus* protocols for protoplasting and transformation by using *pyrG89* as the selective marker were modifications of refs. 19 and 20. Recipient *pyrG89* strains were grown in liquid YG medium (0.5% yeast extract, 2% glucose, and trace elements) supplemented with vitamins, 10 mM uracil, and 5 mM uridine (UU). Putative pyr$^+$ transformants were selected on solid YG medium (with 2% agar in bottom, 1% in overlays, 1 M sucrose, without UU), either at 30°C or by selection for pyr$^+$ and ts$^+$ at 42°C. Transformation procedures for *S. macrospora* were as in ref. 4.

Abbreviations: DAPI, 4,6-diamidino-2-phenylindole; HU, hydroxy urea; Gts, calculated generation times.

§To whom reprint requests should be addressed. E-mail: zickler@igmors.u-psud.fr.

The publication costs of this article were defrayed in part by page charge payment. This article must therefore be hereby marked "*advertisement*" in accordance with 18 U.S.C. §1734 solely to indicate this fact.

Plasmids. We used: pANscos1 (*HygR*; ref. 21); pPL6 (=pPyrG; ref. 22); pRG3 (*pyr-4*; ref. 23); pBimD1 (*bimD*; ref. 6); pDH1 (*SPO76*) and pDH13 (*SPO76-GFP*; ref. 4). For the construction of pGW1454, a 6.7-kb *Nco*I-*Sma*I fragment from pBimD1 was cloned into pBR328 *Eco*RV-*Nco*I; for pGW1460, enhanced green fluorescent protein (EGFP) was amplified from pEGFP-1 (CLONTECH) and inserted into the *Xho*I site of pGW1454; for pGW1463, a 1.4-kb 3′-*Bgl*II/*Xho*I *bimD* cDNA fragment was cloned into the expression vector pQE32 (Qiagen, Chatsworth, CA) *Bam*HI-*Sal*I. The *Escherichia coli* strain DH5α was used as a host in plasmid propagation (24).

Sequencing. A 1.2-kb fragment spanning the *bimD6* mutation was amplified by PCR by using gene-specific primers on genomic DNA from strains WG542 and WG540. Genomic DNA was isolated as described (25). PCR products were sequenced directly with gene-specific primers (4). For DNA sequencing, we used the Dyedeoxy Terminator, Cycle Sequencing kit (Applied Biosystems) and a 373 DNASequencer (Applied Biosystems).

Cytogenetic Methods. For mitotic and cell cycle analyses, conidiospores were either grown in a drop of supplemental minimal medium on a slide or inoculated (5×10^6 per ml) in SM with 50 mM hydroxy urea (HU) and incubated for 13 h at 25°C. After HU treatment, cells were washed twice with SM, and 10 μl samples were taken. C source was glucose (1%) or lactose (3%); N source was 50 mM urea or ammonium. Nuclei were stained with the DNA-specific dye 4,6-diamidino-2-phenylindole (DAPI). For meiotic analyses, fruiting bodies were mechanically squashed with a blunted metal needle.

Cells were processed for immunofluorescence as described for *Sordaria* (26). For BIMD antiserum, *E. coli* $SG_1$3009 cells (Qiagen) were transformed with plasmid pGW1463. After induction with isopropyl-β-D-thiogalactopyranoside, the fusion protein was purified from the bacterial cell lysate by affinity chromatography on a nickel column (Qiagen) and dialyzed against PBS (140 mM NaCl/10 mM sodium phosphate, pH 7.3). Antiserum 560 was raised against the fusion protein in a rabbit, affinity-purified as described (27), and used in a dilution corresponding to 1:200 diluted serum. Secondary antibody was CyTM3 anti-rabbit (Jackson ImmunoResearch), diluted 1:4,000. Cells incubated with primary or secondary antibodies alone gave no signal. Three BIMD-GFP transformants (of WG546 with pGW1460) were analyzed. Cells were observed on a Zeiss Axioplan microscope with images captured by a charge-coupled device Princeton camera.

Western Blot Analysis. For crude protein extracts of *A. nidulans*, mycelium grown at permissive temperature was powdered in liquid nitrogen in the presence of the complete miniprotease inhibitor mixture (Boehringer, no. 1836153), boiled in electrophoresis sample buffer, and centrifuged. Proteins extracted from 7 mg of mycelium were loaded per 3.5-cm-wide slot of a 10% polyacrylamide gel and electrophoresed in parallel with molecular weight markers (Bio-Rad). Of each lane, 0.5 cm was stained with Coomassie blue, and the remainder was transferred to nitrocellulose. After immunoblotting, markers and mycelial proteins were detected with Ponceau S. Binding of BIMD antibodies to 0.3-cm-wide strips was detected by goat–anti-rabbit secondary antibodies conjugated to alkaline phosphatase and incubation in nitroblue tetrazolium chloride/5-bromo-4-chloro-3-indolyl-phosphate, as described (27).

Results

BIMD Localizes to Chromosomes During Mitosis and Meiosis. We determined the localization of BIMD by using both affinity-purified antibodies and a fully functional BIMD-GFP-tagged derivative. The antibody preparation recognizes a single prominent protein species of ≈170 kDa in wild-type extracts, corresponding to a predicted BIMD molecular mass of 166 kDa. The corresponding signal is absent in *bimD6* (Fig. 1*A*); thus, the antibodies are specific for BIMD.

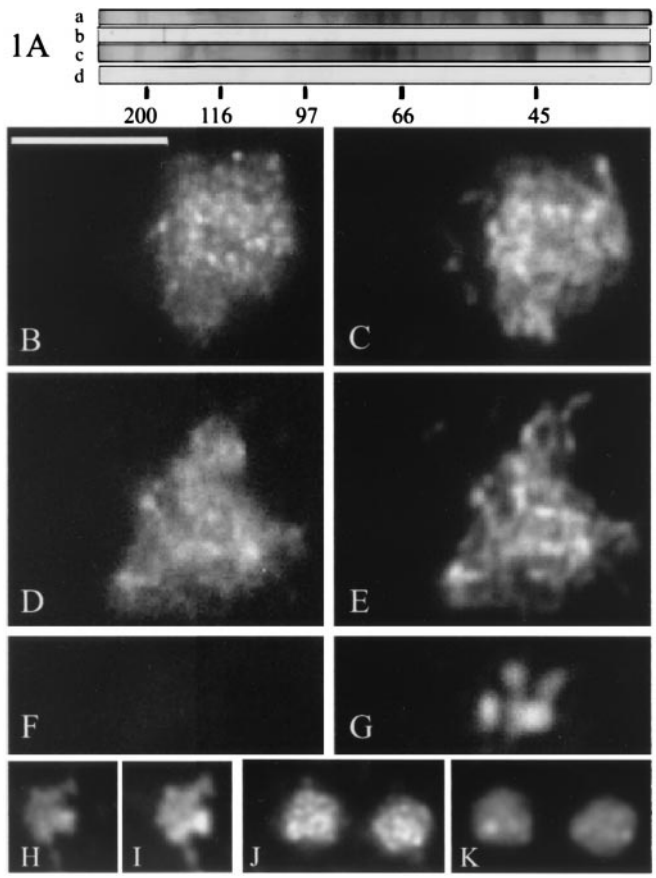

Fig. 1. Localization of BIMD. (*A*) Immunoblot analysis of proteins extracted from wild-type (lanes a and b) and *bimD6* (lanes c and d) mycelium, by using antibodies against the C terminus of BIMD. Lanes a and c, Coomassie blue-stained gels; lanes b and d, corresponding immunoblots probed with affinity-purified anti-BIMD antibodies from serum 560. Molecular size standards are indicated below lane d in kilodaltons. (*B–E*) Wild-type early meiotic prophases (leptotene/zygotene): (*B*) stained with affinity-purified anti-BIMD antibodies from serum 560; (*C*) corresponding DAPI; (*D*) stained with GFP; and (*E*) corresponding DAPI. (*F* and *G*) Metaphase I nucleus stained with (*F*) GFP and (*G*) DAPI. (*H–K*) Mitotic prophase nuclei in wild-type germlings stained with (*H*) GFP and (*J*) anti-BIMD antibodies. *I* and *K* are the corresponding DAPI. (Bars = 5 μm.)

By both approaches, BIMD was observed exclusively in nuclei and, within those nuclei, specifically on chromatin. During meiosis, BIMD is chromosome-associated during prophase I (e.g., Fig. 1 *B–E*) but disappears from the chromosomes as they emerge from the diffuse stage into diplotene (e.g., at metaphase I, Fig. 1 *F* and *G*). It reappears on the chromosomes at telophase(s). Likewise, during mitosis, BIMD dissociates from chromosomes in prometaphase and reassociates at telophase. BIMD was present on the chromatin in resting conidia (G_0 or G_1), in HU arrested cultures (S phase) and in mitotically cycling nuclei (500 germlings observed) (Fig. 1 *H–K*). However, slight differences in staining intensity were discernible at different stages (e.g., brighter in S than in G_1/G_0). In dividing nuclei of mitosis and meiosis, antibody staining detects numerous tiny foci, whereas GFP staining seems more continuous (Fig. 1, compare *B* and *H* with *D* and *J*). These minor differences might reflect different sensitivities of the two techniques. No BIMD-antibody staining was detected in *bimD6* resting or dividing nuclei at either temperature.

The temporal pattern of BIMD localization to chromosomes

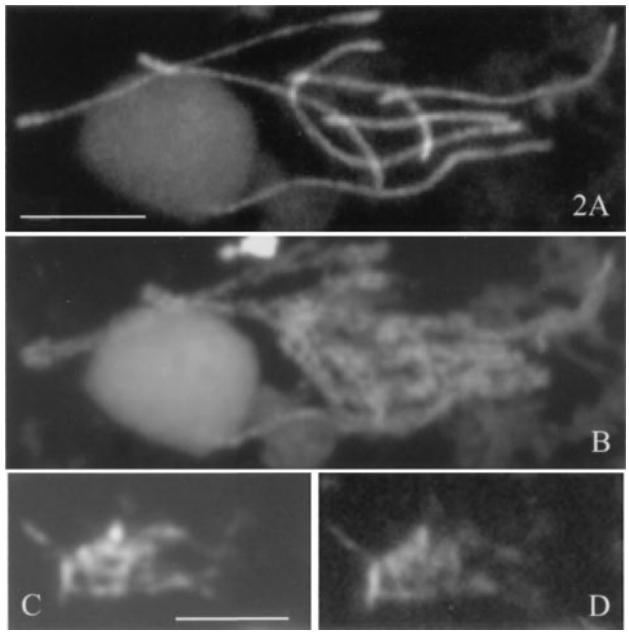

Fig. 2. (*A*) Spread pachytene nucleus of *S. macrospora*: Spo76-GFPp decorates the axes of the synapsed homologs (gray ball, nucleolus). (*B*) Corresponding DAPI. (*C*) DAPI of a spread *A. nidulans* pachytene. (*D*) Corresponding BIMD-GFP stains the entire chromatin mass. (Bars = 5 μm.)

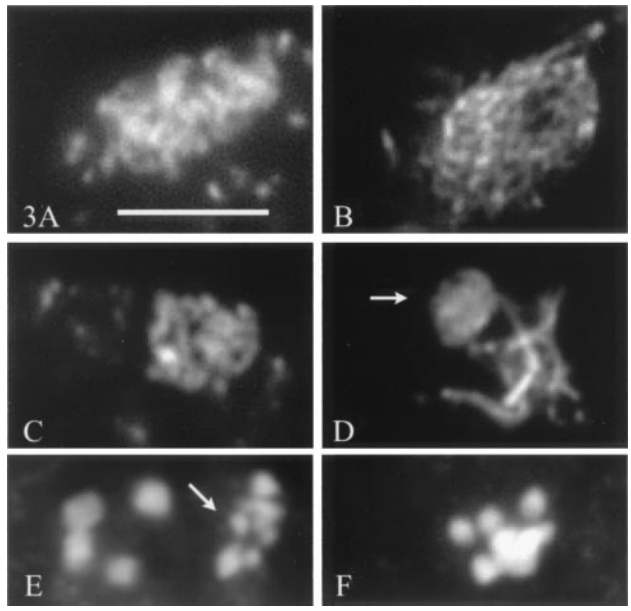

Fig. 3. Progression of meiosis in *bimD6* and wild-type asci. All nuclei are stained with DAPI. (*A*) Early *bimD6* prophase. (*B*) Early wild-type prophase. (*C*) *bimD6* pachytene. (*D*) Wild-type pachytene; arrow indicates the nucleolar organizer bivalent. (*E*) Spread metaphase I nucleus of *bimD6*. Note the small size of some of the chromatin units (arrow) when compared with normal bivalents (four seen, *Left*). (*F*) Wild-type metaphase I (four clearly separated and four overlapping bivalents). (Bar = 5 μm.)

in *A. nidulans* is identical to that found for Spo76p in *S. macrospora* (4). However, two interesting qualitative differences in staining patterns are observed, both during meiotic prophase. First, in *Sordaria*, prophase nuclei are more brightly stained than any other nuclei of either vegetative or sexual cycles (4), which is not the case in *Aspergillus* (Fig. 1, compare *D* and *J*). Second, Spo76p is preferentially localized along the chromosome axes at prophase (Fig. 2 *A* and *B*), whereas BIMD staining does not reveal any axes but instead stains all chromatin (Fig. 2 *C* and *D*).

Unexpected Nature of the *bimD6* Mutation. *bimD* is an essential gene, and *bimD6* was mapped to its 5′ region (6). Sequence analysis of this region in *bimD6* and wild type revealed a single sequence difference: a T to *A* mutation at position 420 in the ORF, which changes the codon TA*T* (Tyr) to TA*A* (Stop). The most straightforward consequence would be the production of a short truncated protein (≈15 kDa) containing the first 140 N-terminal amino acids. Translational readthrough or reinitiation could give a longer polypeptide (reviewed by ref. 28); however, antibodies against (approximately) the C-terminal third of the BIMD protein do not detect any prominent new polypeptide in extracts of *bimD6* (above). Thus, residual function of the BIMD6 protein might reside in the short N-terminal region or be provided by a rather low level of an (undetected) longer protein. Alternatively, *Aspergillus* BIMD may be essential only at high temperature (analogous to *pds1*; ref. 29).

Meiotic Defects of *bimD6*. At permissive temperature, *bimD6* fruiting bodies are comparable to those of wild type in number and morphology, but they remain barren. Wild-type fruiting bodies contain hundreds of asci, within which meiosis occurs. Mutant fruiting bodies contain only few asci (average 10), which indicates that *bimD* function is required during premeiosis. Moreover, *bimD6* asci are abnormal in several respects. (*i*) During prophase I, the chromatin appears always more diffuse in *bimD6* than in wild-type nuclei (Fig. 3, compare *A* and *B*), and a typical pachytene stage with orderly condensed chromosomes is not observed (Fig. 3, compare *C* and *D*). (*ii*) Thirty-three percent of all observed asci (65/200) were in metaphase I (a stage rarely seen in wild type, probably because of its short duration), and only 3% progressed beyond metaphase I, even in older fruiting bodies. The remaining 64% asci were at pachytene or diffuse stage. (*iii*) Metaphase I nuclei exhibit higher numbers of chromatin units than the eight bivalents seen in wild type (Fig. 3, compare *E* and *F*). These units should correspond either to prematurely separated homologs and/or to precociously separated sister chromatids. Because of their small sizes (arrow in Fig. 3*E*), the latter is more likely. However, all analyzed metaphase I nuclei also contained some regularly sized bivalents (Fig. 3*E Left*).

BimD6$^+$ Function Is Required During Early S Through M and Not in G_1 Phases of the Mitotic Cycle. Execution points for *bimD6*$^+$ function were evaluated by germination tests of haploid conidia (in G_1/G_0) by using HU arrest in combination with temperature shifts.

HU arrest *per se* has no effect on the mutant phenotype at either temperature; the same is true for wild-type conidia. In *bimD6* conidia maintained in HU at permissive temperature for 13 and 19 h and then released at permissive temperature, all ensuing mitoses were normal (500 analyzed). When conidia were maintained in HU at restrictive temperature throughout (13 h) and then released at restrictive temperature, they exhibited the same catastrophic mitosis observed in the absence of HU treatment (300 analyzed). For HU arrest in combination with temperature shifts, four different conditions were tested. (*i*) In conidia arrested with HU at permissive temperature and then shifted to restrictive temperature on release of arrest, all mitoses ($n > 400$) were catastrophic in *bimD6* but not in wild type, indicating the existence of an essential function(s) for *bimD* during early S through M. (*ii*) When *bimD6* conidia were arrested at restrictive temperature with HU (13 h), then shifted to permissive temperature still in HU (6 h), and then released at permissive temperature, almost all (over 95%) ensuing mitoses were normal (200 analyzed). Thus BIMD does not play an essential role before the HU-arrest point. (*iii*) When *bimD6* conidia were arrested at restrictive temperature with HU for 13 h and then released at permissive temperature, almost all (over 95%)

ensuing mitoses were catastrophic (200 analyzed). These two latter experiments together indicate that BIMD function is irreversibly inactivated by high temperature. (*iv*) When arrested at restrictive temperature with HU for a longer time (19 h) and then released at permissive temperature, almost all conidia were blocked earlier, before the onset of mitosis (300 analyzed): this experiment indicates that BIMD may play a role during S phase or HU arrest.

BIMD Is a Negative Regulator of Cell Cycle Progression. We also asked whether BIMD might have a general role in cell cycle regulation. *Aspergillus* germination tubes are well suited for analysis of cell cycle kinetics (14). Each tube is a single cell that develops from a uninucleate haploid conidium (see Fig. 5*A*, which is published as supplemental data on the PNAS web site, www.pnas.org) by the progressive occurrence of sequential mitotic divisions (Fig. 5*B*). The nuclei within each tube divide synchronously; concomitantly, the tube elongates, and its 2, 4, 8, or more nuclei migrate to spatially specific positions after each division (Fig. 5 *C–E*). The cell cycle history of each germling can thus be deduced from the size of the tube and the number and position of its nuclei.

Wild-type and *bimD6* germlings were compared at permissive temperature, where normal mitoses occur in both strains, and were examined for four mitotic cycles. For each strain, at each time point analyzed, 200–400 germlings were scored. Three protocols were examined. First, conidia were germinated after cold storage, which provides some degree of synchrony, in SM + glucose and urea. Compared with wild type, *bimD6* cycles faster: its first mitosis occurs earlier, and the number of nuclei per sample increases faster (Fig. 4*A*). By linear regression analysis, calculated generation times (Gts) were 2 h 21 and 2 h 59 for *bimD6* and wild type, respectively. The difference between these values is statistically significant ($P < 0.05$; Fig. 4*B*). Second, an even greater difference was observed when cold-stored conidia were germinated in SM with a less favorable combination of C- and N-sources (lactose + urea): Gts were 6 h 28 for *bimD6* and 9 h 14 for wild type ($P < 0.1$). Third, conidia were synchronized with HU, and only one division was followed: Gts calculated for this division were of 7 h 49 for *bimD6* and 13 h 46 for wild type ($P < 0.05$). Thus, *bimD6* nuclei consistently divided earlier and cycled faster than wild type; furthermore, the extent of the difference increases in parallel with the length of the cycle.

Importantly, however, whereas *bimD6* exhibits faster nuclear divisions, it maintains normal coordination between nuclear divisions and other aspects of germination, such that the entire cellular program proceeds faster than normal (Fig. 4*C*). Each step of germination is faster in *bimD6* than in wild type (Fig. 4 *C1–T16*). In particular, initiation of tube formation after the first division is faster in *bimD6* (as seen Fig. 4*C* by the percentage of conidia with two nuclei in *C2* compared with binucleate tubes in *T2*). At later stages, tube elongation occurs with an essentially normal delay after completion of the corresponding nuclear divisions. Wild-type and mutant tube lengths were, respectively, 19 ± 4 and 17 ± 5 μm when tubes contained two well separated nuclei (as in Fig. 5*D*) and 25 ± 6 and 23 ± 7 μm when they contained four nuclei (Fig. 5*E*; 100 analyzed). The nuclear migration process, however, is not perfectly normal in *bimD6*. For example, after the second mitosis, the four nuclei of wild-type germlings are usually distributed uniformly throughout the tube (Fig. 5*E*); in four nucleated *bimD6* germlings, in contrast, 30% had not yet started tube formation (Fig. 5*F*) or contained randomly distributed nuclei (Fig. 5*G*). Also, the average distance between nuclei, although variable in both strains, was smaller in *bimD6* than in wild type. Thus, coupling of nuclear migration to nuclear division appears less strict in *bimD6.*

***bimD6* Is Defective for Interhomolog, but Not Intrachromosomal, Recombination.** *bimD6* mutants show increased sensitivities to methyl methanesulfonate and UV only during germination and not in quiescent conidia (6). Germinating conidia of *bimD6* also

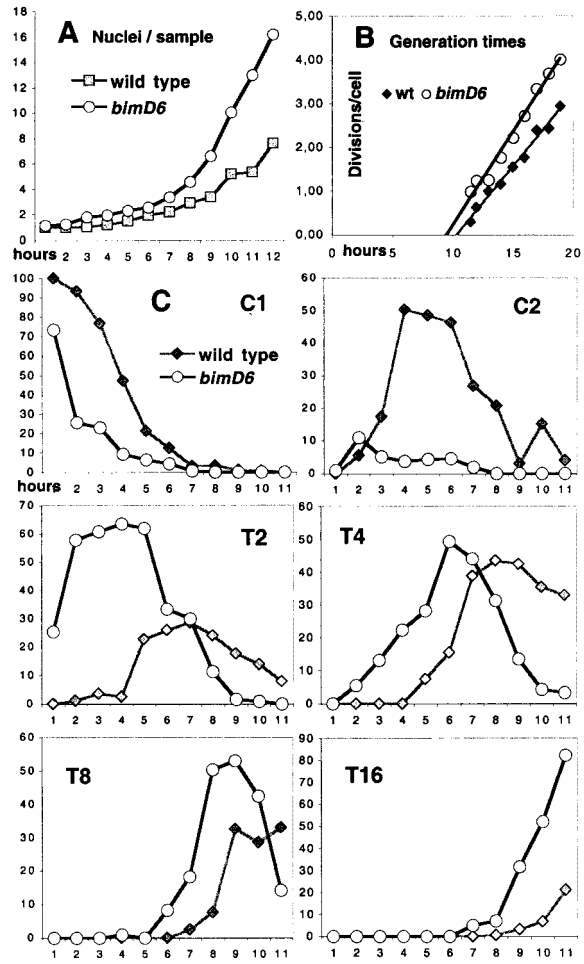

Fig. 4. Rate of mitoses and germling phenotypes in *bimD6* and wild-type conidia germinated in SM (glucose + urea) during 20 h. (*A*) Number of nuclei per sample. Samples were analyzed every hour, and hour 1 in graph corresponds to the start of divisions, namely at 8 h after inoculation of the conidia. (*B*) For each time point (*X*), the average number of divisions per cell (*Y*) was calculated by logarithm (average number of nuclei per cell)/logarithm 2. After linear regression ($Y = bX$), Gt was determined by using the equation $Gt = 1/b$; 300–2,000 nuclei were analyzed for each time point. (*C*) Wild-type phenotypes are indicated by gray squares and lines, whereas *bimD6*s (m) are given as black curves with plain circles; C1 and C2 represent, respectively, the percentage of uninucleated and binucleated conidia, and T2–T16 correspond to the percentage of germ tubes with 2, 4, 8, or 16 nuclei.

showed x-ray sensitivity (2- to 2.5-fold; see Fig. 6, which is published as supplemental data on the PNAS web site, www.pnas.org). To further probe the role of BIMD for repair, we examined *bimD6* for spontaneous mitotic recombination, which is thought to occur in response to endogenous DNA damage. We analyzed in parallel the *Aspergillus* mutant *uvsC114*, defective for a *recA/RAD51* homolog (25); *uvsC114* is also sensitive to radiation and methyl methanesulfonate only while dividing (30).

Well-developed genetic systems for assessment of mitotic recombination are available in *Aspergillus* (30). We selected for rare ad^+ recombinants arising in diploids heterozygous for the two distinguishable alleles *adE8* and *adE20* (ref. 16; Table 1). Because of the unusually close linkage of outside markers to *adE*, the fraction of ad^+ recombinants that have undergone crossing over of flanking markers can be determined; more specifically, genetic analysis of haploid segregants reveals the arrangement of markers on the two homologs. Both *bimD6* and *uvsC114* reduce

Table 1. Allelic recombination in *adE8*/*adE20* diploids: Absolute frequencies of recombinants and relative frequencies of conversion vs. crossing over

	Control (+)	*bim*D6	*uvsC114*
Absolute frequencies of $ad^+ \times 10^{-6}$	11.43 ± 1.33	1.22 ± 0.21	1.20 ± 0.35
Class* Convertants/Crossovers	Relative frequencies of recombination types		
Single conversions†	77%	78%	82%
Single crossovers	13%	15%	11%
Two events: Conversion and/or CO	7%	5%	5%
Multiple events	3%	2%	2%
Total of ad^+ recombinants analyzed	30	53	44

*Classification of ad^+ recombinants was done as in ref. 16.
†*adE8*→+ or *adE20*→+.

the frequency of ad^+ recombinants in *adE8*/*adE20* diploids about 9-fold (Table 1 and Table 2, which is published as supplemental data on the PNAS web site, www.pnas.org). However, among these recombinants, the relative frequencies of crossover and noncrossover types resemble those of wild type (Table 1). This result contrasts with findings for two other *Aspergillus* DNA repair mutants, *musN227* (hyperrec) and *musL222* (hyporec), both of which exhibit an increased ratio of crossover to noncrossover recombinants (16).

We also tested both *bimD6* and *uvsC114* for intrachromosomal "gene conversion" within a duplication. We used a *pyrG89* strain with a heterozygous direct repeat of benomyl resistant (*benA22*) and sensitive ($benA^+$) alleles separated by intervening *pyr-4* and plasmid sequences (17). On growth-reducing concentrations of benomyl, this heterozygous *benA22*/$benA^+$ duplication strain shows intermediate resistance to benomyl; however, fully resistant sectors can arise by recombination (Fig. 7, www.pnas.org). When selection for *pyr-4* function is maintained, all resistant sectors result from conversion of $benA^+$ to *benA22* without loss of the intervening *pyr-4* segment. Such conversions can reflect intrachromatid and/or intersister events. Unexpectedly, *bimD6* duplication strains were considerably more sensitive to benomyl than wild type or *uvsC114* (see Table 3, www.pnas.org). Therefore, we assayed recombination at reduced benomyl concentrations for *bimD6* (0.96 μg/ml) instead of 1.2 μg/ml used for wild-type/*uvsC114*. Under these conditions, *bimD6* shows about as many resistant sectors as the control, whereas *uvsC114* produced none (Fig. 7, www.pnas.org). Thus, whereas *uvsC114* reduces conversion between interrupted *benA22*/$benA^+$ repeats, *bimD6* has no influence on this type of mitotic recombination.

The *S. macrospora SPO76* Gene Complements the Heat and Methyl Methanesulfonate (MMS) Sensitivities of *A. nidulans bimD6* but Not the Meiotic Defects. Wild-type versions of either *SPO76* or *bimD* were introduced into a *bimD6, pyrG89* double mutant recipient by cotransformation with pyr^+ plasmids. In each case, a considerable fraction of transformants exhibited complementation for both heat and MMS sensitivity: 26/77 for *SPO76* and 34/54 for *bimD*. Analysis of six *bimD* transformants that exhibited complementation for mitotic defects revealed that meiotic defects were also complemented. In contrast, among 16 of the mitotically complemented *SPO76* transformants, none showed complementation of *bimD6* meiotic defects; in three of these cases, the presence of *SPO76* was confirmed by Southern blotting. Analogously, in the reciprocal test, complementation of the meiotic defects of *spo76–1* in *S. macrospora* was observed only after transformation with *SPO76* and not after transformation with *bimD* (respectively, 25/51 and 0/786).

Discussion

The findings presented above confirm and extend the analogy between BIMD and Spo76p and provide information regarding the basic roles of the Spo76 family proteins.

Strong Analogies Between BIMD and Its Orthologs. First, BIMD, like Spo76p, is abundant and chromosome-associated at all stages of the mitotic and meiotic programs except from end of prophase to telophase. Analogously, human PDS5 is chromatin associated during interphase and in mitosis, during prophase and telophase (11). In contrast, budding yeast Pds5p is seen on chromatin in G_1 (low signal), S into mitosis (strong signals) until onset of chromatid separation (9, 10). Thus, in *Aspergillus*, *Sordaria*, and vertebrates, the protein dissociates from the chromosomes earlier than in budding yeast. An attractive hypothesis is to link this finding with the differences in chromosome condensation between these organisms (see refs. 9 and 11 for discussion). Second, *SPO76* (4) and *bimD* (here) are required for cohesion during both mitotic and meiotic programs. Pds5p is found essential for mitotic sister cohesion establishment and maintenance (9, 10); a similar latter effect could explain why *bimD6* is highly benomyl sensitive at permissive temperature (above). Third, Spo76p, BIMD, and Pds5p are also required for normal chromosome compactness during mitosis (refs. 4 and 9, here) and meiosis (ref. 4, here). Fourth, *spo76–1* and *bimD6* are sensitive to DNA-damaging agents (refs. 6 and 8, here). Finally, complementation analysis shows that *SPO76* and *bimD* are functional homologs with respect to their roles in mitotic chromosome metabolism.

BIMD Is a Negative Regulator of Normal Mitotic Cell Cycle Progression. We show that *bimD6* cycles significantly faster than wild-type. Rapid cycling is observed for all aspects of germ tube development, with normal or nearly normal coupling retained between nuclear and extranuclear processes. Our results therefore imply that an abundant chromosome-associated protein is involved in modulating normal cell cycle progression. Moreover, because cycling is faster in *bimD6* than in wild type, BIMD appears to be a negative regulator of cell cycle progression, i.e., BIMD is part of a mechanism that normally constrains cell cycle progression in circumstances where a slower rate of cycling is more appropriate. That overexpression of *bimD* causes a fully reversible arrest in G_1 (6) further supports this interpretation. Because the exact nature of the *bimD6* mutation is not known, its phenotype may, however, not reflect simply elimination of gene function.

We have not determined which stage(s) of the cell cycle are affected, but the only period when BIMD is not on the chromosomes, metaphase/anaphase, is normally so brief (13) that changes in these stages are clearly not the primary effect. We find it attractive to think that the major effect is during G_1 or early S phase. First, overexpression of *bimD* in wild-type cells results in a block at the G_1 or early S phase of the cell cycle (6). Second, a greater difference in Gts between *bimD6* and wild type was seen in poorer medium, and in several organisms, variations in nutrient conditions affect specifically the duration of G_1 (31–33). Third, cell cycle modulation at G_1 would fit with the tumor suppressor role of the human ortholog *AS3:* in prostrate cells, up-regulated expression of the *AS3* gene mediates androgen-induced G_1 arrest (5). In accord with these possibilities, BIMD protein is seen in G_1 nuclei. With respect to its essential function(s), however, BIMD is not required

before the HU arrest point, as shown by experiments involving HU arrest in combination with temperature shifts. Likewise, yeast Pds5p function is not required during G_1 (9). *bimD6* may (also) influence progression through S phase. The most prominent difference in Gts between *bimD6* and wild type was found when HU was used to synchronize germlings. The continued effect of HU (after removal) could be explained by a slowing of DNA replication, e.g., because the cell needs time to replicate over DNA lesions (34).

How could proteins like BIMD/Spo76p, whose primary role is to mediate chromosome morphogenesis, also be implicated in the cell cycle progression? They could remodel chromatin, for example, by providing (direct or indirect) intrachromatid crosslinks. This remodeling could define chromatin domains to be activated/repressed, for example in the vicinity of genes involved in cyclin D expression during G_1 (33). Likewise, such crosslinks could define which chromosome region should be searched for repair from S through G_2 (below) and/or mark at which chromosome regions sister-chromatid cohesion should be established during S phase (35).

BIMD Determines the Probability of Interhomolog Mitotic Recombination. The absolute frequency of spontaneous allelic interhomolog recombination is strongly reduced in *bimD6,* but the distribution of recombinants into crossover and noncrossover classes among such recombinants is the same as in wild type. This phenotype suggests that *bimD6* affects the probability that an interhomolog event will occur at all; once that decision has been made, the recombination process proceeds as usual. This interpretation is supported by the fact that intrachromosomal recombination is normal in *bimD6*, suggesting that BIMD may not be involved in the enzymology of recombinational repair *per se*.

Why is recombinational repair reduced in *bimD6*? Several other mutants defective in sister chromatid cohesion are also radiation sensitive and/or defective in DNA double strand break repair (reviewed in ref. 36). In budding yeast, cohesins bind to regularly spaced preferential positions that likely correspond to the AT-queue of the chromosome axis (37), and Pds5p binds to the same sites (9). We therefore suggest that BIMD may be required for recombination events that occur in the context of the chromosome axis. For example, BIMD could mark which chromatin loops have to be searched on the sister or the homolog as a template for recombinational repair. When some of those landmarks are missing, as for example in *bimD6,* safety mechanisms may prevent or reduce recombinational repair. On the other hand, intrachromosomal repair between repeated sequences apparently does not depend on those landmarks. Both *bimD6* and the *rad21–45* mutant of *Schizosaccharomyces pombe* (38, 39) are highly sensitive to DNA-damaging agents but have no defect in mitotic recombination between interrupted direct repeats. An analogous phenotype, decreased interhomolog recombination with no effect on intrachromosomal recombination, was also observed during budding-yeast meiosis in the *hop1* and *red1* mutants, which are defective in axis-associated components (40, 41). That direct repeat recombination is independent of Hop1 and Red1p (42) could imply that also in meiosis, this type of recombination does not occur in the context of the chromosome axis.

BIMD Localization and Function Mirror Atypical Features of Meiosis in *A. nidulans*. Although BIMD and Spo76p play functionally analogous roles in mitosis, their meiotic roles may differ in accord with several "atypical" aspects of meiosis in *A. nidulans*. First, the meiotic localization of the two proteins is different. Spo76p is most abundant during *Sordaria* meiotic prophase and assembles in strong lines along chromosome axes during synapsis (4). BIMD, in contrast, is not or only slightly more abundant during *Aspergillus* meiosis, and it does not reveal defined axes during prophase I. These differences are likely related to differences in underlying chromosome structure and/or function and may also explain the lack of heterologous complementation of meiotic defects. *Sordaria* forms synaptonemal complexes (43), whereas *A. nidulans* appears to lack these structures (44). Moreover, with respect to meiotic chromosome function, *A. nidulans* differs from *Sordaria* (43) by its lack of positive crossover interference (review in ref. 18). On the basis of the proposition that crossover interference involves the imposition and relief of stress along the chromosomes (45), it was argued that Spo76p might be a transducer of the disruptive chromosomal forces that provide the necessary stress (4). If this hypothesis is correct, the need for a robust axis and a stress-transducing protein would be greater in an organism that exhibits crossover interference than in an organism in which this process is absent, thus explaining the differences between Spo76p and BIMD localization and, more generally, between axial development in organisms with and without interference.

We are grateful to Françoise James for expert technical assistance. We thank Greg May (University of Texas, Houston, TX) and Berl Oakley (The Ohio State University, Columbus) for the gift of strains and plasmids. We particularly thank Nancy Kleckner and the reviewers for helpful suggestions. This work was supported by the Netherlands Organisation for Scientific Research (D.v.H.), by European Economic Community contract CHRXCT 94 0511 (to C.H. and D.Z.), by a research grant from the Natural Science and Engineering Research Council of Canada (to E.K.), and by the Centre National de la Recherche Scientifique (UMR 8621 to D.Z.).

1. Yang, J. & Kornbluth, S. (1999) *Trends Cell. Biol.* **9,** 207–210.
2. Nasmyth, K. (1996) *Science* **274,** 1643–1645.
3. Zou, H., McGarry, T. J., Bernal, T. & Kirschner, M. W. (1999) *Science* **285,** 418–422.
4. van Heemst, D., James, F., Pöggeler, S., Berteaux-Lecellier, V. & Zickler, D. (1999) *Cell* **98,** 261–271.
5. Geck, P., Maffini, M. V., Szelei, J., Sonnenschein, C. & Soto, A. M. (2000) *Proc. Natl. Acad. Sci. USA* **97,** 10185–10190.
6. Denison, S. H., Kafer, E. & May, G. S. (1992) *Genetics* **134,** 1085–1096.
7. Darwiche, N., Freeman, L. A. & Strunnikov, A. (1999) *Gene* **233,** 39–47.
8. Moreau, P. J. F., Zickler, D. & Leblon, G. (1985) *Mol. Gen. Genet.* **198,** 189–197.
9. Hartman, T., Stead, K., Koshland, D. & Guacci, V. (2000) *J. Cell Biol.* **151,** 613–626.
10. Panizza, S., Tanaka, T., Hochwagen, A., Eisenhaber, F. & Nasmyth, K. (2000) *Curr. Biol.* **10,** 1557–1564.
11. Sumara, I., Vorlaufer, E., Gieffers, C., Peters, B. & Peters, J. M. (2000) *J. Cell Biol.* **151,** 749–761.
12. Holt, C. L. & May, G. S. (1996) *Genetics* **142,** 777–787.
13. Bergen, L. G. & Morris, N. R. (1983) *J. Bacteriol.* **156,** 155–160.
14. Fischer, R. (1999) *FEMS Microbiol. Rev.* **23,** 39–68.
15. Pontecorvo, G., Roper, J. A., Hemmons, L. M., MacDonald, K. D. & Bufton, A. W. J. (1953) *Adv. Genet.* **5,** 141–238.
16. Zhao, P. & Kafer, E. (1992) *Genetics* **130,** 717–728.
17. Dunne, P. W. & Oakley, B. R. (1988) *Mol. Gen. Genet.* **213,** 339–345.
18. Kafer, E. (1977) *Adv. Genet.* **19,** 33–131.
19. Debets, F. & Bos, K. (1986) *Fungal Genet. News Lett*. **33,** 24.
20. Osmani, S. A., May, G. S. & Morris, N. R. (1989) *J. Cell Biol.* **104,** 1495–1504.
21. Osiewacz, H. D. (1994) *Curr. Genet.* **26,** 87–90.
22. Oakley, B. R., Rinehart, J. E., Mitchell, B. L., Oakley, C. E., Carmona, C., Gray, G. L. & May, G. S. (1987) *Gene* **61,** 385–399.
23. Waring, R. B., May, G. S. & Morris, N. R. (1989) *Gene* **79,** 119–130.
24. Hanahan, D. (1983) *J. Mol. Biol.* **166,** 557–580.
25. van Heemst, D., Swart, K., Holub, E. F., van Dijk, R., Offenberg, H. H., Goosen, T., van den Broek, H. W. J. & Heyting, C. (1997) *Mol. Gen. Genet.* **254,** 654–664.
26. Thompson-Coffe, C. & Zickler, D. (1984) *Dev. Biol.* **165,** 257–271.
27. Lammers, J. H. M., Offenberg, H. H., van Aalderen, M., Vink, A. C. G., Dietrich, A. J. J. & Heyting, C. (1994) *Mol. Cell. Biol.* **14,** 1137–1146.
28. McCarthy, J. E. G. (1998) *Microbiol. Mol. Biol. Rev.* **62,** 1496–1553.
29. Yamamoto, A., Guacci, V. & Koshland, D. (1996) *J. Cell Biol.* **133,** 99–110.
30. Kafer, E. & May, G. S. (1998) in *DNA Damage and Repair,* eds. Nickoloff, J. A. & Hoekstra, M. F. (Humana, Totowa, NJ.), Vol. 1, pp. 477–502.
31. Silje, H. H. W., Schure, E. G., Rommens, A. J. M., Huls, P. G., Woldringh, C. L., Verkleij, A. J., Boonstra, J. & Verrips, C. T. (1997) *J. Bacteriol.* **179,** 6560–6565.
32. Carlson, C. R., Grallert, B., Stokke, T. & Boye, E. (1999) *J. Cell. Sci.* **112,** 939–946.
33. Riou-Khamlichi C., Menges, M., Healy, J. M. & Murray, J. A. (2000) *Mol. Cell. Biol.* **20,** 4513–4521.
34. Paulovitch, A. G. & Hartwell, L. H. (1995) *Cell* **82,** 841–847.
35. Wang, Z., Castano, I. B., DeLasPenas, A., Adams, C. & Christman, M. F. (2000) *Science* **289,** 774–779.
36. van Heemst, D. & Heyting, C. (2000) *Chromosoma* **109,** 10–26.
37. Blat, Y. & Kleckner, N. K. (1999) *Cell* **98,** 249–259.
38. Fortuno, E. A., Osman, F. & Subramani, S. (1996) *Mutat. Res.* **364,** 147–160.
39. Subramani, S. (1991) *Mol. Microbiol.* **5,** 2311–2314.
40. Hollingsworth, N. M. & Byers, B. (1989) *Genetics* **121,** 445–462.
41. Rockmill, B. & Roeder, G. S. (1990) *Genetics* **126,** 563–574.
42. Mao-Draayer, Y., Galbraith, A. M., Pittman, D. L., Cool, M., Malone, R. E. (1996) *Genetics* **144,** 71–86.
43. Zickler, D., Moreau, P. J. F., Huynh, A. D. & Slezec, A. M. (1992) *Genetics* **132,** 135–148.
44. Egel-Mitani, M., Olson, L. W. & Egel, R. (1982) *Heriditas* **97,** 179–187.
45. Kleckner, N. (1996) *Proc. Natl. Acad. Sci. USA* **93,** 8167–8174.